Strong photoluminescence of nanostructured crystalline tungsten oxide thin films

M. Feng, A. L. Pan, H. R. Zhang, Z. A. Li, F. Liu, H. W. Liu, D. X. Shi, B. S. Zou, and H. J. Gao[a)]
Nanoscale Physics and Devices Laboratory, Institute of Physics, Chinese Academy of Sciences, Beijing, 100080, China

(Received 12 October 2004; accepted 18 February 2005; published online 29 March 2005)

Strong photoluminescence (PL) is observed in nanostructured crystalline tungsten oxide thin films that are prepared by thermal evaporation. Two kinds of films are investigated—one made of nanoparticles and another of nanowires. At room temperature, strong PL emissions at ultraviolet-visible and blue regions are found in both of the films. Compared with the complete absence of emission of bulk phase tungsten oxide powder under the same excitation conditions, our results clearly demonstrate the quantum-confinement-effect-induced photoluminescence in nanostructured tungsten oxides. © *2005 American Institute of Physics*. [DOI: 10.1063/1.1898434]

Tungsten oxide has been extensively studied for distinctive physical and chemical properties—especially the electrochromic, photochromic, gaschromic properties—in recent years.[1–4] Much effort has been made to probe the mechanism of chromism,[5,6] the coloration efficiency,[7,8] the photocurrent process,[9–12] and the absorption properties[13] of tungsten oxide thin films. Nevertheless, less attention has been paid to the emission properties of WO_3 since it is an indirect-gap semiconductor with low emission efficiency. Manfredi *et al.*[11] reported light emission in thin WO_3 films at liquid nitrogen temperatures. However, the emission disappears at room temperature, showing photoluminescence in tungsten oxide is not preferred at room temperature. Here we report on a strong photoluminescence found in nanostructured crystalline tungsten oxide thin films at room temperature. Two kinds of films (*P* films and *W* films, *P* films are referred to as the films composed of nanoparticles and *W* films are referred to as the films composed of nanowires) are involved in the investigation. Under excitation at 256 nm, *P* films exhibit strong ultraviolet-visible (UV) emission at 355 nm, and *W* films show two emission peaks at 355 and 475 nm. In contrast, from bulk phase WO_3 powder, no photoluminescence was detected under the same excitation conditions.

Both the films were prepared through simple thermal evaporation. A spiral coil made up of a tungsten wire (99.9%, 0.3 mm in diameter) was used as the evaporation source. Before curled into coil, the wire was burnished and cleaned with ultrasonication. In a vacuum system, a Si(111) wafer as a substrate was heated to 400 °C before evaporation. Then 5 A current was introduced to flow through the coil at a vacuum of 2×10^{-3} Pa. *P* films and *W* films can be obtained by controlling experimental conditions. X-ray diffraction (XRD) data were obtained on a Rigaku D/MAX 2400 type spectroscope (Cu K_1, wavelength: 1.5406 Å). A field-emission type scanning electron microscope (SEM) (XL-SFEG, FEI Corp.) and transmission electron microscope (TEM) (Hitachi 9000) were used to study structures of the films. X-ray photon spectroscopy (XPS) was measured with an ESCALAB-5 photoelectron spectrometer using a monochromic MgK anode (1253.6 eV). PL spectra measurements were conducted at room temperature on an Edinburgh Analytical Instruments F900 Emscan 2-320, with a Xe lamp as the excitation source.

XRD analysis on the two types of films clearly indicates that both the thin films have good crystalline structure. As shown in Fig. 1, the reflection peaks of the *P* films correspond to standard peaks of WO_3 (JCPDS card No: 85-2460), while the reflection pattern of *W* films indicates that the crystalline structure matches the reflection of $W_{18}O_{49}$ (JCPDS card No: 84-1516). Since no additional oxygen was introduced into the system, the origin of the tungsten oxides on the substrate might be due to the WO_3 on the wire that was not removed totally in the cleaning process. When we used the same spiral coil that has been already evaporated for the first time as the second and third evaporation source, almost nothing could be found on the substrate, thus demonstrating our speculation. In the experiments, the *W* films were prepared with longer evaporation time of about 80 s and the radiation from the lighted coil may greatly increase the substrate temperature, resulting in a loss of oxygen and formation of a $W_{18}O_{49}$ tungsten oxide structure. Usually, we get amorphous films if the substrate is not heated before evaporation, indicating that high substrate temperature is helpful for formation of crystalline tungsten oxide structures.

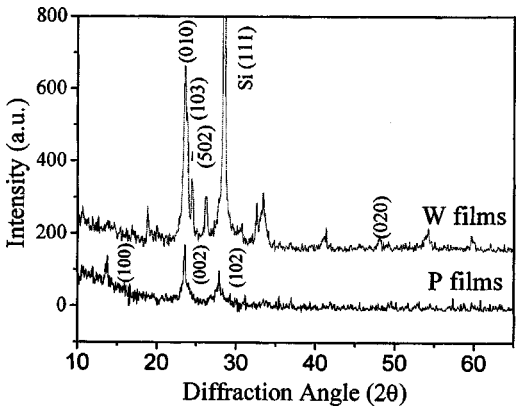

FIG. 1. XRD patterns for the *P* films sample and the *W* films sample, showing both the *P* films and *W* films are crystalline—corresponding to WO_3 and $W_{18}O_{49}$ diffraction patterns, respectively.

[a)]Author to whom correspondence should be addressed; electronic mail: hjgao@aphy.iphy.ac.cn

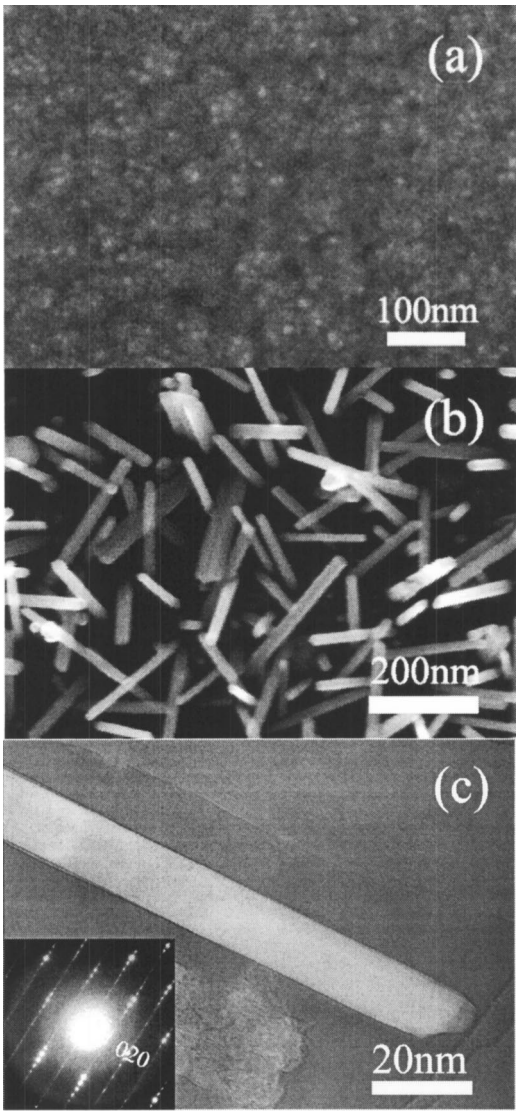

FIG. 2. Morphologies and structures of the prepared tungsten oxides films. (a) SEM image of *P* films, showing small particles of the film. (b) SEM images of *W* films, indicating disperse nanowires. (c) TEM image of a single nanowire, the inset image is the SAD pattern, respectively.

Figure 2 shows the SEM images of the two kinds of films obtained. One can see the *P* films are made of small particles of about 10 nm in diameter [Fig. 2(a)], while the *W* films are mainly of disperse nanowires with a diameter about 20 nm and various lengths [Fig. 2(b)]. The average thickness of the *P* and *W* thin films were determined with a SEM and an atomic force microscope to be about 30 nm. Figure 2(c) is a typical bright-field TEM image of a nanowire, and the inset image is a selected area diffraction (SAD) pattern. These show clearly that the nanowire is single crystalline and the growth axis is along the $\langle 010 \rangle$ $W_{18}O_{49}$ direction, both in good agreement with the x-ray diffraction analysis. Those streak-like SAD spots along directions perpendicular to the $\langle 010 \rangle$ growth axis imply there are modulated structures in the $W_{18}O_{49}$ nanowires, which is caused by crystallographic shear planes or partial oxygen vacancy walls.[14] It has been found that the coil's position relative to the substrate has a great effect for preparing *P* films and *W* films. When the substrate is dead against the tungsten coil, *P* films of particles are formed. However, if the coil is not dead against the wire, i.e., the coil is shifted to the side of the substrate—we get *W* films. Considering the different flux density of the evaporated tungsten oxides because of different relative orientations of the substrate and the coil, relatively smaller flux density can be the reason for the formation of dispersed nanowires. Another different detail in the preparation of the two films is the evaporation time. *P* films are prepared with larger flux density and shorter time (20 s), while *W* films are obtained with smaller flux density and longer time (80 s).

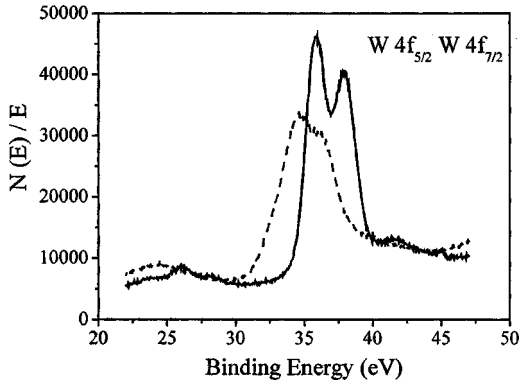

FIG. 3. W_{4f} level XPS for the *P* films (solid) and the *W* films (dash), indicating W^{6+} valence state of *P* films and mixed valence states of *W* films.

In order to understand the composition of the different tungsten oxide films, we used XPS to investigate the valence distribution of both the tungsten oxide films. As shown in Fig. 3, the XPS spectrum of the *P* films shows double peaks with the binding energies of 35.6 and 37.7 eV, corresponding to $W_{4f\ 7/2}$ and $W_{4f\ 5/2}$, respectively.[6] They are the typical valence state peaks of W^{6+} and are consistent with the standard spectra of WO_3. This result fits well with the XRD analysis of the *P* films. On the other hand, there is a broad peak in the XPS pattern of *W* films showing obvious mixed states in the sample.

Strong photoluminescence (PL) emission for both films was observed, while no emission was found on commercial WO_3 powder. At the same time, no obvious emission peak was observed for a treated bare Si plate by putting a bare Si wafer in the vacuum system and heating it to the same reaction temperature. Thus, the possibility of emission from the substrate is ruled out. Figure 4(a) shows PL spectra of the *P* films and the *W* films excited at 256 nm. A very clear emission peak at 355 nm was observed in the PL spectra of *P* films, while two PL emission peaks were observed at 355 and 435 nm from *W* films. Figure 4(b) is the emission spectra of the *P* films excited under different wavelengths, 256, 275, and 309 nm. The emission of the Si substrate is provided for comparison with tungsten oxide films. It can be seen that the emission peak at 355 nm does not shift under different excitation wavelengths and shows intrinsic properties of the film itself.

WO_3 is an indirect-gap semiconductor and has very low emission efficiency. It is believed that in the bulk crystal of indirect-gap materials, the electron-hole combination is possible only through phonon emission or absorption for the wave vector compensation. However, in nanoscale indirect-gap semiconductors such as Si, Ge, room-temperature photoluminescence has been observed. Studies about this photoluminescence reveal quantum-confinement-induced indirect-to-direct gap conversion in the nanostructures, strongly suggesting the importance of the quantum-confinement effect in the luminescence process.[15,16] Recently, Lee[17] reported PL

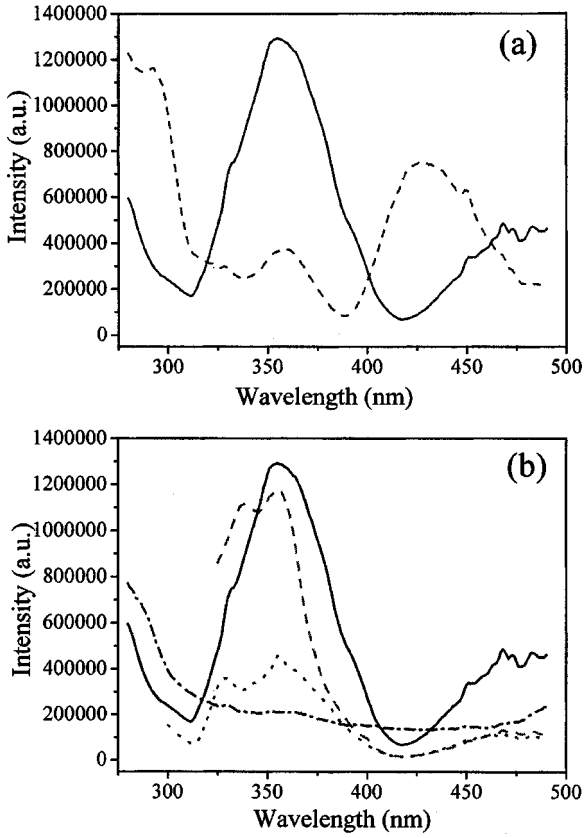

FIG. 4. PL spectra of the nanostructured crystalline thin films. (a) Emission spectra of the *P* films (solid) and *W* films (dash) on the substrate excited at 256 nm. (b) PL of the *P* films excited at different wavelength: 256 nm (solid), 275 nm (dot), 309 nm (dash), and the emission spectra of the Si substrate (dash dot) excited at 256 nm (the intensity has been multiplied by 1.5).

emissions at 344 and 437 nm from $W_{18}O_{49}$ nanorods in $CHCl_3$ solution at room temperature. The diameter of the nanorods ranges from 3 to 7.5 nm. In our studies, the UV emission peak at 355 nm is longer than the 344 nm peak observed by Lee. But the 435 nm of the blue emission is close to the 437 nm reported. Considering the smaller diameter of the nanorods, the shorter UV emission observed from them may come from the quantum-confinement-effect on the band gap, implying a quantum-confinement-effect in these tungsten oxides nanostructures. For the *P* films, no blue emission was detected. Since the composition of the *P* films is WO_3, we can deduce reasonably that the blue emission disappears because of minor oxygen vacancies in the *P* films. Thus, the two emissions observed may also be attributed to the band–band transition and oxygen vacancies or defects, as proposed by Lee.

In summary, we report strong photoluminescence in nanostructured crystalline tungsten oxide thin films at room temperature. By controlling experimental conditions, crystalline tungsten oxide thin films composed of different nanostructures can be obtained through thermal evaporation of tungsten wire. An UV emission at 355 nm and a blue emission at 435 nm are observed on the prepared nanostructured crystalline thin films. These emission peaks can be attributed to band–band transition and localized states induced by the presence of oxygen vacancies or defects in the nanostructure. Since no PL can be detected in bulk phase material, it is helpful for understanding the quantum-confinement effect on the band structure of this kind of indirect-band gap semiconductors and the photoluminescence process in them.

The authors thank M. Dotson for critical reading of the manuscript. The project is partly supported by the National Natural Science Foundation of China, National "863" and "973" programs of China and the Chinese Academy of Sciences.

[1] J. D. Guo and M. S. Whittingham, Int. J. Mod. Phys. B **7**, 4145 (1997).
[2] P. A. Gillet, J. L. Fourquest, and O. Bohnke, Mater. Res. Bull. **27**, 1145 (1992).
[3] J. D. Guo, Y. J. Li, and M. S. Whittingham, J. Power Sources **54**, 461 (1995).
[4] Y. Zhao, Z. C. Feng, and Y. Liang, Sens. Actuators B **66**, 171 (2000).
[5] R. Hurditch, Electron. Lett. **11**, 142 (1975).
[6] M. Sun and N. Xu, J. Mater. Res. **15**, 927 (2000).
[7] C. Bechinger, M. S. Burdis, and J. G. Zhang, Solid State Commun. **101**, 753 (1997).
[8] S. H. Lee, H. M. Cheong, C. E. Trancy, and S. K. Deb, Appl. Phys. Lett. **75**, 1541 (1999).
[9] J. Hao, S. A. Studenikin, and M. Cocivera, J. Appl. Phys. **90**, 5064 (2001).
[10] S. Benci, M. Manfredi, and G. C. Salviati, Solid State Commun. **33**, 107 (1980).
[11] M. Manfredi, C. Paracchini, G. C. Salviati, and G. Schianchi, Thin Solid Films **79**, 161 (1981).
[12] C. Santato, M. Odziemkowski, M. Ulmann, and J. Augustynski, J. Am. Chem. Soc. **123**, 10639 (2001).
[13] S. K. Deb, Philos. Mag. **27**, 801 (1973).
[14] J. Sloan, J. L. Hutchison, R. Tenne, Y. Feldman, T. Tsirlina, and M. Homyonfer, J. Solid State Chem. **144**, 100 (1999).
[15] T. Takagahara and K. Takeda, Phys. Rev. B **46**, 15578 (1992).
[16] A. N. Khold, V. L. Shaposhnikov, N. Sobolev, and S. Ossicini, Phys. Rev. B **70**, 035317 (2004).
[17] K. Lee, W. S. Seo, and J. T. Park, J. Am. Chem. Soc. **125**, 3408 (2003).